

New copolymers of *N,N*-dimethylacrylamide with blocked isocyanates for oligonucleotide immobilization in DNA microarray technology

M. Viganò^{a,*}, M. Levi^a, S. Turri^a, M. Chiari^b, F. Damin^b

^a *Dipartimento di Chimica, Materiali e Ingegneria Chimica "Giulio Natta", Politecnico di Milano, Piazza Leonardo da Vinci 32, 20133 Milan, Italy*

^b *Istituto di Chimica del Riconoscimento Molecolare, CNR, Via Bianco, 20100 Milan, Italy*

Received 15 February 2007; received in revised form 14 May 2007; accepted 14 May 2007

Available online 18 May 2007

Abstract

A family of copolymers of *N,N*-dimethylacrylamide containing blocked isocyanate functionalities is presented. The copolymers were characterized by DSC, GPC and ¹H NMR. Calorimetric analysis showed for any composition broad endothermic phenomena followed by a stronger exothermic peak, which can be attributed, respectively, to the deblocking and subsequent reaction of generated NCO groups.

Characterization of glass slides coated with these polymers was done by contact angle measurements and atomic force microscopy. While the former method revealed minimal differences with formation of moderately hydrophilic surfaces, microscopic images showed a more homogeneous coating formation for the copolymer structure with 50% molar of blocked isocyanate. The efficiency of the coated substrates in the immobilization of amino functionalized oligonucleotides was successfully assessed through binding tests and analysis by confocal fluorescence microscopy.

Finally, some model microarrays were fabricated by spotting and hybridization with complementary, fluorescently labelled targets was carried out. It resulted in surfaces coated with copolymers which show well defined circular spots with a fluorescence intensity higher than that obtained by slides treated by silanization, and based on the same immobilization chemistry.

© 2007 Elsevier Ltd. All rights reserved.

Keywords: Blocked isocyanate; Coating; DNA microarray

1. Introduction

In recent years DNA microarray technology has been widely studied and developed as a fast and accurate tool for advanced diagnostics [1–5]. Microarray technology allows the analysis of many genes simultaneously, working with small volumes and reduced times, thus providing information on nucleic acid sequences in a faster, simpler and cheaper way than with traditional methods.

DNA microarrays can be fabricated according to two different main methods: in situ synthesis by photolithographic techniques [6–11], and mechanical deposition by ink-jet printing, spotting or split-pin technology [6,7,12–16]. The quality

of the microarray is defined by a large number of parameters, like spot and probe density, background noise and spot morphology, durability, and ease of processing [6]. All these parameters are largely influenced by the chosen DNA immobilization chemistry.

One of the main problems of microarrays is the limited storage stability of the functionalized support materials, affecting the reproducibility of results and so requiring other chemical steps to regenerate reactive groups [17,18]. Different strategies for surface functionalization have been reported [7] which varies considerably for the different approaches and applications. Silanization with formation of a polyorganosiloxane layer with reactive functionalities, such as epoxides, amines and aldehydes, is the classical approach followed to attach covalently oligonucleotides to the surface [19,20]. The silanization process is very flexible, rather cheap and advantageous because it enables the introduction of diversified functional

* Corresponding author. Tel.: +39 0223993275.

E-mail address: marco.vigano@polimi.it (M. Viganò).

groups. However, a strict control of operative conditions is needed for a good reproducibility of results and to achieve a homogeneous monolayer or few layer deposition. Although covalent immobilization density varies in the range 10^{11} – 10^{13} molecules cm^{-2} [7], only 40–50% of the surface-bond probe is usually hybridized with the target [19].

As an alternative to silanization, dendrimeric structures and polymer functional coatings can be used in order to increase oligonucleotide density and fluorescent signals and, therefore, to amplify the sensitivity of detection [21,22]. These types of structures can improve microarray efficiency because it is supposed that the macromolecular character reduces the steric hindrance during covalent immobilization and hybridization due to the higher distance between functional groups [23].

Among the various chemical functionalities available, blocked isocyanates [24–26], well known and used in many surface coatings applications, show the advantage of quite a long shelf life because the active NCO groups are masked and protected. Therefore surfaces functionalized with blocked isocyanates can be safely stored and thermally deactivated just before use. In a preceding work of ours [27] this functionality was directly grafted onto a glass slide surface by a standard silanization procedure. The model microarray obtained provided excellent results in terms of binding and hybridization efficiency [27], making blocked isocyanates good candidates for the preparation of high performance DNA microarray substrates.

In this work a series of new copolymers obtained from 2-isocyanatoethyl methacrylate (IEM) blocked with methyl ethyl ketoxime (MEKO) and *N,N*-dimethylacrylamide (DMA) were synthesized and characterized. These copolymers were then applied onto glass slides and some model DNA microarrays were fabricated by spotting technology. Finally, the effective performances were evaluated through binding and hybridization tests.

2. Experimental part

2.1. Materials

N,N-Dimethylacrylamide (DMA), isocyanate ethyl methacrylate (IEM), toluene, methyl ethyl ketoxime (MEKO), dibutyltin dilaurate (DBTDL), α,α' -azoisobutyronitrile (AIBN), tetrahydrofuran (THF) and untreated glass microscope slides ($25 \times 75 \text{ cm}^2$) were all purchased from Sigma (St. Luis, MO). THF was distilled, degassed and stored over dry molecular sieves before.

Ethanolamine and sodium dodecyl sulphate (SDS) were supplied from Merck (Darmstadt, Germany). Oligonucleotides, 23-mer amino modified at the 5' terminus, 23-mer Cy3-oligonucleotides labelled at the 5' terminus and 23-mer Cy3-oligonucleotides amino modified at 3' terminus and labelled at the 5' terminus were purchased from MWG-Biotech AG (Ebevsberg, Germany). Tris[hydroxymethyl]aminomethane (Tris) was from Promega (Madison, USA). NaCl and sodium citrate were from Serva (Heidelberg, Germany).

2.2. Blocked isocyanate monomer synthesis

All glasswares were oven dried at 120 °C overnight and reactions were carried out under purified nitrogen atmosphere. A droplet of DBTDL was added to IEM (0.01% w/w). The mixture was degassed by alternating vacuum and nitrogen purge for a few minutes, then it was kept under magnetic stirring at 60 °C. Successively, MEKO (10% molar excess) was added dropwise. The scheme of reaction is reported in Fig. 1a. The reaction mixture was kept at 60 °C until the free isocyanate groups were blocked (checked by FTIR spectroscopy monitoring the disappearance of $-\text{NCO}$ stretching band at about 2260 cm^{-1}).

2.3. Copolymer synthesis

MEKO blocked isocyanate ethyl methacrylate (IEMB in the following), DMA and AIBN (0.1% mol/mol on IEMB + DMA) were dissolved in dry THF (30% w/w solution) in a round-bottom flask equipped with condenser, magnetic stirring and nitrogen connection. The reaction mixture was degassed by alternating vacuum and nitrogen purge for a few minutes and kept at 70 °C under nitrogen for 24 h. Different monomer feeds as high as 10, 30, 50 and 70% (expressed as $\text{mol}_{\text{IEMB}}/\text{mol}_{\text{DMA+IEMB}}$) were copolymerized. They were indicated in the following as CO10, CO30, CO50 and CO70. The homopolymer of IEMB (polyIEMB) and DMA (polyDMA) were also prepared in the same way. Fig. 1b reports the general copolymerization scheme.

The copolymers were precipitated using toluene as non-solvent. They were then again solubilised in THF and reprecipitated (this procedure was repeated three times in order to purify the polymers and remove the residual monomers which are soluble in toluene). The purification of CO10 copolymer was carried out at 0 °C in order to facilitate the phase separation of the polymer which is partially soluble in toluene at room temperature.

2.4. Polymer characterization

^1H NMR was performed in deuterated chloroform (CDCl_3) using a Bruker AC 300 spectrometer, working at 300.133 MHz. Calculations were made with MestRe-C software. Relative molecular weights were determined by gel permeation chromatography (GPC) using a Waters 510 instrument, equipped with a refractive index detector, Waters 410 differential refractometer, and a set of 4 Waters Styragel HR columns packed with crosslinked styrene–divinylbenzene copolymer particles (porosity 10^2 – 10^5 \AA). THF was used as eluent at 30 °C and GPC chromatograms were calibrated with standard polystyrene samples. The FTIR spectra of the samples were recorded using a Thermo-Nicolet FTIR Nexus infrared spectrometer with a nominal resolution of 4 cm^{-1} . Differential scanning calorimetry (DSC) was carried out with a Mettler-Toledo DSC 823° instrument, with the following thermal cycle: first heating from -50 °C to 280 °C , cooling

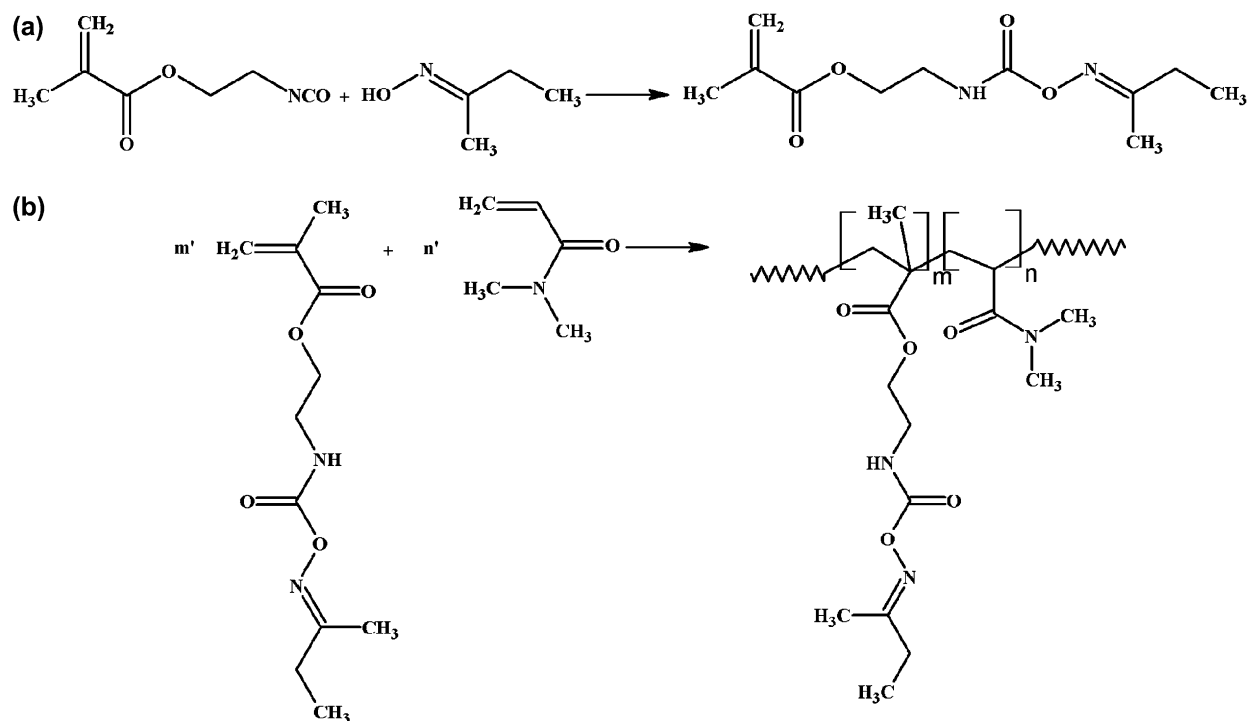


Fig. 1. (a) Blocking reaction of IEM with MEKO. (b) Copolymerization of DMA and IEMB; $m/n = 0$ to ∞ .

from 280 °C to –50 °C and second heating from –50 °C to 250 °C (rate 10 °C/min).

2.5. Glass slide coating

Microscope glass slides (2.5 × 7.5 cm) were accurately cleaned according to the following dipping procedure: ethanol for 30 min, 1 M NaOH solution for the next 30 min, rinsing with distilled water, drying, 1 M HCl solution for another 1 h, rinsing again with distilled water, drying. The cleaned glass slides were dip-coated into a THF polymer solution for 30 min at room temperature. Concentrations of 1 and 0.1% w/w were used. After coating the slides were let air-dry and then stored in a dry environment until use.

2.6. Surface characterization

Static contact angles (CA) were performed with an OCA20 instrument (Dataphysics Co., Germany), equipped with a CCD fotocamera and with a 500 μL-Hamilton syringe to dispense liquid droplets. Measurements were made at room temperature by means of the sessile drop technique. At least 10 measurements were performed at different places on each sample and results were averaged. Bidistilled water was used as probe liquid and the delivered volume was 1.25 μL. Contact angle data were carried out with time interval of 1 s between drop deposition and the measurement.

Atomic force microscopy (AFM) topographic images were obtained using a NSCRIPTON™ DPNWriter™ (Nanoink, USA) instrument in tapping mode with a resonant oscillating frequency of 320 kHz and commercial silicon tips at ambient

pressure, temperature and humidity. The mean spring constant of these tips was 0.2 N m⁻¹. The mean surface roughness (R_a), which is the average deviation of the surface heights relative to average mean of these peaks in a scanned image, and the root-mean-square roughness (R_{rms}), which is the standard deviation of measured data on the analyzed surface, were calculated according to the following equations:

$$R_a = \frac{\sum_{n=1}^N |z_n - \bar{z}|}{N} \quad (1)$$

$$R_{rms} = \frac{\sum_{n=1}^N (z_n - \bar{z})^2}{N} \quad (2)$$

where \bar{z} is the average mean of measured heights and N is the number of points included in analyzed surface.

2.7. Microarray fabrication and functional tests

2.7.1. Oligonucleotides probe immobilization

Synthetic 23-mer 5'-amine-modified oligonucleotides (100 μM/mL stock solution) were dissolved in 150 mM sodium phosphate buffer of pH 8.5. This solution of oligonucleotides at 10 μM concentration was printed onto coated glass slides to form a 400 spots microarray using a Qarray² spotter (Genetix, UK). Spotting was carried out at +12 °C and 33% humidity. Printed slides were placed in an uncovered storage box, laid in a sealed chamber, saturated with NaCl, and incubated overnight. The glass supports coated with the polymers were previously deblocked and then incubated at room temperature. The deblocking reaction was carried out at

180 °C under vacuum. After incubation, all residual reactive groups of the glass surface were eliminated by dipping the slides in 50 mM ethanolamine/0.1% SDS/0.1 M Tris pH 9.0 at 50 °C for 15 min (10 mL of this blocking solution for each slide). Then, the slides were washed two times with water and dipped for 15 min in 4 × SSC/0.1% SDS buffer, pre-warmed at 50 °C and rinsed with water and dried.

2.7.2. Hybridization with complementary oligonucleotides

Complementary 23-mer oligonucleotides labelled at the 5' terminus with Cy3 were dissolved in the hybridization buffer (2 × SSC/0.1% SDS/0.02% BSA) at a concentration of 1 μM and immediately spread to microarray spotted area (2.5 μL/cm² of coverslip applied on treated zone). The slides were placed in the hybridization chamber, laid in a humidified incubator at 65 °C for at least 2 h. Afterwards, the slides were shaken in 4 × SSC at room temperature to remove the coverslip and then they were washed twice for 5 min with 2 × SSC/0.1% SDS solution, prewarmed at hybridization temperature. This operation was followed by other two washings with 0.2 × SSC and 0.1 × SSC, both carried out at room temperature for 1 min. Finally, the slides were dried using a centrifuge and so they were ready to be scanned with confocal laser scanner, ScanArray Lite (Perkin Elmer, MA, USA). Fluorescence signals were measured with the laser power kept constant at 22% and the photomultiplier tube gain at 64%.

2.7.3. Binding test

Ten subarrays (containing each 16 spots) of 5'-amino modified oligonucleotides labelled with Cy3 and dissolved in 150 mM sodium phosphate, pH 8.5, ranging in concentration from 0.5 to 25 μM, were patterned using the Qarray² spotter. Printed slides were first scanned with ScanArray Lite and then placed in an uncovered storage box, laid in a sealed chamber, saturated with NaCl, and incubated overnight with the same procedures used in the hybridization test during immobilization step. After incubation, the washing treatments were applied to the slides with the similar protocols used in the hybridization test during hybridization step but without complementary oligonucleotides in the hybridization buffer. Fluorescence signals were measured with the laser power kept constant at 20% and the photomultiplier tube gain at 75%.

3. Results and discussion

Strangely enough, isocyanates were so far scarcely used for biomacromolecules immobilization [28], although NCO groups are in principle highly reactive with many hydrogen active functions like –NH₂, –OH and –SH. All these groups are easily introduced or already present in biomacromolecules like DNA and proteins.

One drawback of isocyanates is the excessive moisture sensitivity of the NCO-functionalized surface, which could lose its functionality upon storage. A possible solution is to mask this functional group with a blocking agent which can be thermally removed before use, as normally done in coating and adhesive technology [24–26]. In a preceding work of ours

[27] it was demonstrated that ketoxime blocked isocyanates can be used as functional groups for the fabrication of DNA microarrays by silanization.

In light of this the aim of the present work was to incorporate blocked isocyanate functions within a copolymer structure in order to improve the quality and performances of the resulting microarray. Several copolymers with different compositions were therefore synthesized by free radical polymerization and characterized (Fig. 1b), and some results are shown in Table 1.

By analyzing Table 1 data it can be seen that except for the case of CO10 composition, all yields are around 60%, while M_w 's vary between 50 000 and 70 000 g/mol. The anomalous low yield and high M_w value of CO10 could be due to the loss of low molecular weight fraction of the polymer, which is partially soluble in toluene even at low temperature.

Fig. 2 compares the FTIR spectra of the homopolymers and copolymers obtained. Band at 1720 cm⁻¹ is attributed to urethane C=O stretching, and it is indicative of the presence of IEMB monomer, while band at 1620 cm⁻¹ (tertiary amide C=O stretching) is a marker for DMA. In a certain range of composition, to be determined experimentally, the relative intensities of these IR bands could give information about the copolymer composition, however, a more accurate and quantitative analysis was done by ¹H NMR (Fig. 3). The integrated area of the peaks attributed to CH₂ (2 hydrogens) in α to the NH group of PolyIEMB (3.5 ppm) and to the two CH₃ (6 hydrogens) groups of PolyDMA (2.8 ppm) were used to calculate the effective molar percentage of IEMB monomer in the copolymer according to the following relation:

$$\%_{\text{IEMB}} = \frac{\frac{A_{3.5 \text{ ppm}}}{H_{3.5 \text{ ppm}}}}{\frac{A_{3.5 \text{ ppm}}}{H_{3.5 \text{ ppm}}} + \frac{A_{2.8 \text{ ppm}}}{H_{2.8 \text{ ppm}}}} \times 100 \quad (3)$$

In Eq. (3) $A_{3.5 \text{ ppm}}$ and $A_{2.8 \text{ ppm}}$ are, respectively, the areas of the peak at 3.5 and 2.8 ppm, and $H_{3.5 \text{ ppm}}$ and $H_{2.8 \text{ ppm}}$ are the relative number of hydrogens.

The composition data are shown in Table 1 along with yield and molecular weight values.

As far as thermal properties are concerned, Fig. 4 shows as an example of the whole DSC cycle carried out for CO50

Table 1
Monomer feed composition, effective copolymer composition, yield and weight-average molecular weight (M_w) of the copolymers CO10, CO30, CO50 and CO70, and for the homopolymers PolyIEMB and PolyDMA

Polymer	Monomer feed composition ^a (%)	Copolymer composition ^{a,b} (%)	Yield (%)	M_w by GPC (g/mol)
PolyIEMB	100	—	56.5	49 120
CO70	70	68.8	61.3	59 710
CO50	50	53.6	62.6	67 920
CO30	30	36.3	58.7	72 310
CO10	10	18.4	26.5	108 670
PolyDMA	0	—	61.2	63 200

^a mol_{IEMB}/mol_{DMA+IEMB}.

^b Calculated via ¹H NMR.

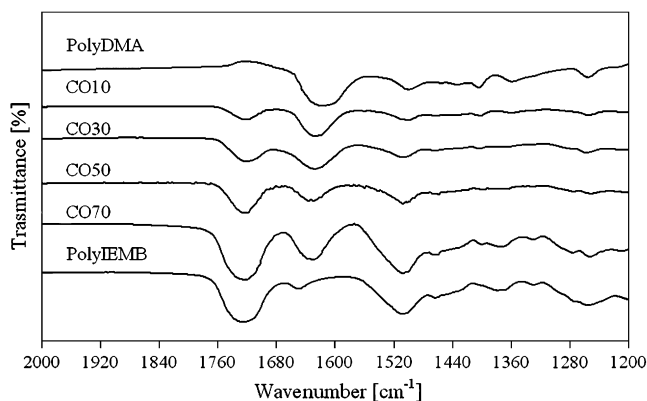


Fig. 2. FTIR spectra of PolyDMA, CO10, CO30, CO50, CO70 and PolyIEMB from 2000 to 1200 cm^{-1} .

product. The DSC traces for all the other copolymers and for PolyIEMB are qualitatively similar, and calorimetric data are summarized in Table 2. In the first heating run from -50 to 280 $^{\circ}\text{C}$ the T_g of CO50 at 39 $^{\circ}\text{C}$ is first measured, and followed at higher temperature by a former, broad endothermic peak (likely due to the deblocking reaction and the evaporation of the blocking agent) and by a latter, much stronger exothermic peak. By analyzing Table 2 data the independence of such peak temperature from the copolymer's composition is evident. Moreover, its enthalpy change ΔH increases proportionally to the IEMB weight fraction in the copolymer. This suggests that the high temperature exothermic peaks are due to some reactions of the deblocked isocyanates, for example their possible cyclotrimerization or other addition reactions. In this view, however, the ΔH value for PolyIEMB is out of range. This effect is not completely clear and requires further analysis.

The second and third runs (Fig. 4, segments b and c) are flat, without clear evidence of peaks or heat capacity changes. It suggests that during the first run a complete deblocking occurs followed by reaction of all isocyanate groups, crosslinking and likely shift of T_g to higher temperature.

The glass transition values of Table 2 can be fitted as a function of the copolymer composition using different analytical

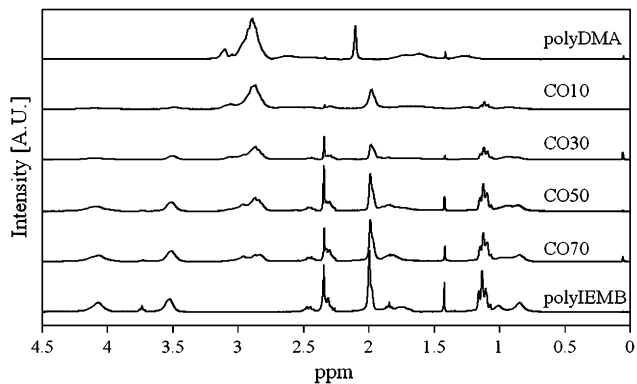


Fig. 3. NMR spectra of PolyDMA, CO10, CO30, CO50, CO70 and PolyIEMB from 4.5 to 0 ppm.

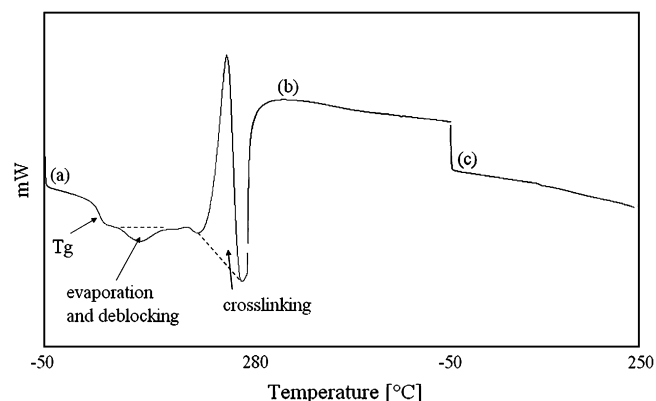


Fig. 4. Complete DSC cycle for CO50: (a) first heating run from -50 to 280 $^{\circ}\text{C}$, (b) cooling run from 280 to -50 $^{\circ}\text{C}$ and (c) second heating run from -50 to 250 $^{\circ}\text{C}$.

relations. The simplest of these is the well-known Fox equation [29]:

$$\frac{1}{T_g} = \frac{w_{\text{IEMB}}}{T_{g,\text{polyIEMB}}} + \frac{w_{\text{DMA}}}{T_{g,\text{polyDMA}}} \quad (4)$$

where w_{IEMB} and w_{DMA} are, respectively, the weight ratio of IEMB and of DMA in the copolymers and $T_{g,\text{polyIEMB}}$ and $T_{g,\text{polyDMA}}$ are, respectively, the glass transition of PolyIEMB and PolyDMA. However, in our case the Fox equation did not give a good fitting (data not shown). Better interpolation was achieved with the Couchman–Karasz equation [30]:

$$\ln(T_g) = \frac{\ln(T_{g,\text{polyIEMB}}) + \left(k \frac{w_{\text{DMA}}}{w_{\text{IEMB}}}\right) \ln(T_{g,\text{polyDMA}})}{1 + \left(k \frac{w_{\text{DMA}}}{w_{\text{IEMB}}}\right)} \quad (5)$$

w_{IEMB} and w_{DMA} being the weight ratio of IEMB and of DMA in the copolymers, $T_{g,\text{polyIEMB}}$ and $T_{g,\text{polyDMA}}$, respectively, the glass transition temperatures of PolyIEMB and of PolyDMA, and k can be considered an adjustable parameter. The Couchman–Karasz plot gave good data fitting when parameter k was set to 0.07 (Fig. 5).

For the following coating experiments PolyIEMB and CO50 compositions were compared. Well-cleaned glass slides

Table 2

IEMB weight ratio, glass transition temperature and crosslinking^a calorimetric data for the copolymers CO10, CO30, CO50 and CO70, and for the homopolymers PolyIEMB and PolyDMA

Polymer	Weight ratio of IEMB (%)	T_g ($^{\circ}\text{C}$)	Crosslinking ^a	
			Peak temperature ($^{\circ}\text{C}$)	ΔH (J/g)
PolyIEMB	100	32.5	249.4	190.88
CO70	84	36.9	249.0	207.12
CO50	74	38.9	256.4	180.20
CO30	58	35.0	247.8	127.86
CO10	35	41.0	255.1	75.56
PolyDMA	0	121.0	—	—

^a With “crosslinking” all the possible reactions among free isocyanates are indicated.

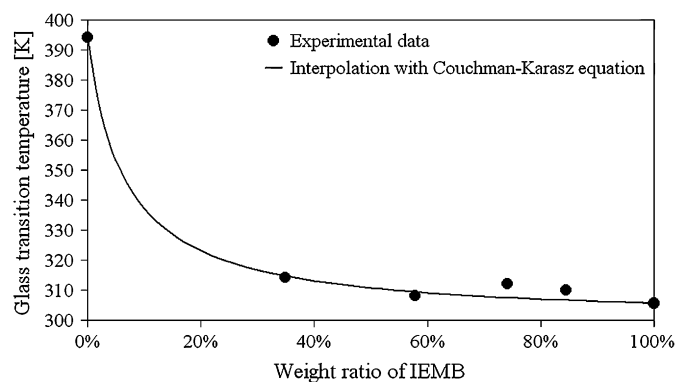


Fig. 5. Glass transition temperature of the polymers as function of the weight ratio of IEMB. The continuous line was obtained using the Couchman–Karasz equation with a value of 0.07 for the parameter k .

were dip-coated for 30 min in a 0.1 and 1% w/w polymer solution in THF. The coated glass slides were dried and characterized through static contact angle measurements, atomic force microscopy, binding and hybridization functional tests.

Static contact angles (Fig. 6) with water showed negligible differences in the moderately hydrophilic behavior of the two polymers: the difference of the mean values is only 1.4° . On the other hand an effect of solution concentration was observed, with an increment of $+10^\circ$ passing from 0.1 to 1% solution concentration. This behavior could be due to the formation of a non-homogeneous coating at high dilution, and in such a case the presence of higher surface tension zones involves a lower contact angle against water.

In contrast to the minor differences in the contact angle measurements, the AFM images of the glass surface coated with PolyIEMB at 1% (PolyIEMB-S-1%) and with CO50 at 1% (CO50-S-1%) appear very different (Fig. 7). The former coating (Fig. 7a) shows the presence of sub-micrometric dewettings with a maximum depth of about 60 nm. Dewettings are typical coating defects caused by a high interfacial tension or by the presence on the surface of islands of lower surface tension [31,32]. As a consequence the homopolymer does not wet completely the substrate [33–35]. The demodulation image of PolyIEMB-S-1% (image not show) does not show, however,

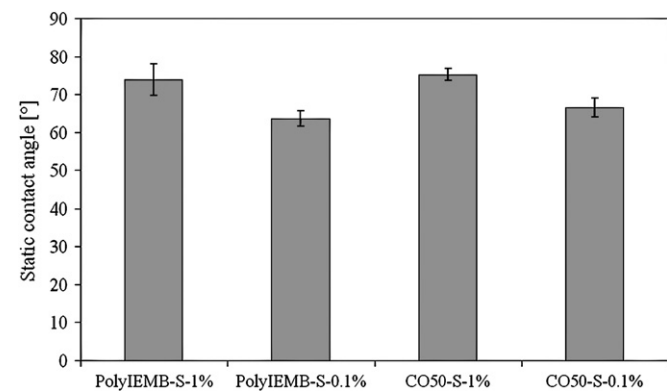


Fig. 6. Static contact angle of PolyIEMB-S-1%, PolyIEMB-S-0.1%, CO50-S-1% and CO50-S-0.1%.

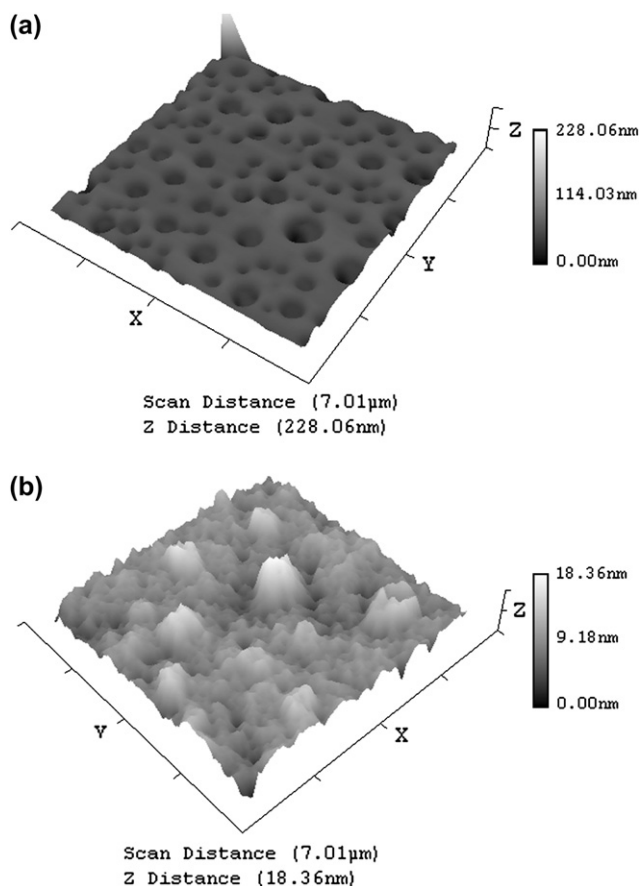


Fig. 7. 3D image of the topography of (a) PolyIEMB-S-1% and (b) CO50-S-1% obtained via tapping mode atomic force microscopy.

any phase difference between peaks and valleys in the dewetting region. This would suggest that only a partial dewetting occurs, but no uncoated glass remains.

The image of CO50-S-1% (Fig. 7b) does not show any dewetting. Surface appears much more homogeneous, with the presence of 10 nm high and 1 μm large protrusions. The better coating capacity of CO50-S-1% is probably due to the presence of DMA. In fact this monomer shows a high affinity towards the glass support which is often exploited in electrophoresis technology [36].

The roughness measured for the coated glass supports are reported in Table 3. For both solution concentrations the surface roughness induced by copolymer coatings is lower than those of homopolymer. This is a further confirmation of the better film forming properties of the CO50 structure. In all cases the roughness of the coatings are higher than those of the untreated glass support ($R_a = 0.23 \text{ nm}$, $R_q = 0.27 \text{ nm}$).

Table 3
Mean surface roughness R_a and root-mean-square roughness R_q for PolyIEMB-S-1%, PolyIEMB-S-0.1%, CO50-S-1%, CO50-S-0.1%

Sample	R_a (nm)	R_q (nm)
PolyIEMB-S-1%	13.37	22.06
PolyIEMB-S-0.1%	23.35	31.36
CO50-S-1%	1.44	2.32
CO50-S-0.1%	17.57	30.99

Finally, the performances of the coated surfaces for DNA immobilization was investigated through binding tests of amino terminated and fluorescently labelled synthetic oligonucleotides. Glass treated substrates were previously thermally activated as explained in the experimental part.

The normalized residual fluorescence, $F = F_w/F_0$ (where F_0 and F_w are the fluorescence intensities before and after the washing treatment as explained in the experimental part), was taken into consideration. The F versus concentration trend of Cy3 amino modified oligonucleotide spots is shown in Fig. 8; curves of coatings at 0.1% are not reported because they were partially detached during the washing procedure. For comparison, results of silanization carried out with the same functional group were included in the graph as reported in a recent work [27].

No significant difference between the fluorescence curves relative to the two polymeric systems can be observed. This result, along with the high value of residual fluorescence for the

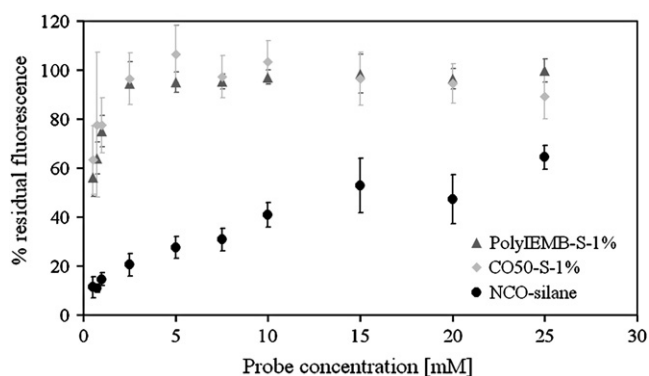


Fig. 8. Residual fluorescence as of the concentration of Cy3 amino modified oligonucleotides for PolyIEMB-S-1%, CO50-S-1% and NCO-silane.

concentration usually used in the hybridization test ($F = 100%$ with concentration as high as $10 \mu\text{M}$), suggests that both types of polymers allow a covalent bonding of the amino terminated oligonucleotides onto the glass substrate. Moreover, for all the concentrations tested of the Cy3 amino modified oligonucleotides, the normalized residual fluorescence of the polymeric coatings is much higher than that obtained from the surface silanized with the same immobilization chemistry [27]. This effect could be due to the increased functional groups availability in the former case. Actually in case of silanized systems the functional group is very close to the surface with formation of a 2D reactive layer. On the contrary in a macromolecular system the functional groups are spatially well distributed and formation of a 3D reactive system is feasible [21,22].

In another set of experiments hybridization of amino functional non-fluorescent oligonucleotide spotted probes has been performed by using the fluorescently labelled complementary targets. Fig. 9 presents the fluorescence microscopy images for (A) PolyIEMB-S-1% and (B) CO50-S-1% coated surfaces, while the corresponding fluorescence intensities are shown in Fig. 10. In contrast to the results observed before, the hybridization intensities of the two polymer systems are now quite different. PolyIEMB-S-1% shows a fluorescence intensity (mean \pm SD = $15\,200 \pm 7470$ AFU) which is lower than those of CO50-S-1% (mean \pm SD = $24\,480 \pm 6032$ AFU). This behavior might be attributed to an excessive number of functional groups onto the surface. A too high density of probes spotted onto the surface could cause problems of steric hindrance: if oligos are too close to each other, the labelled complementary targets are not accessed by the complementary oligonucleotide [37]. Solution concentration apparently does not influence the hybridization ability of the system; actually the fluorescence intensities of PolyIEMB-S-1% and of PolyIEMB-S-0.1% are

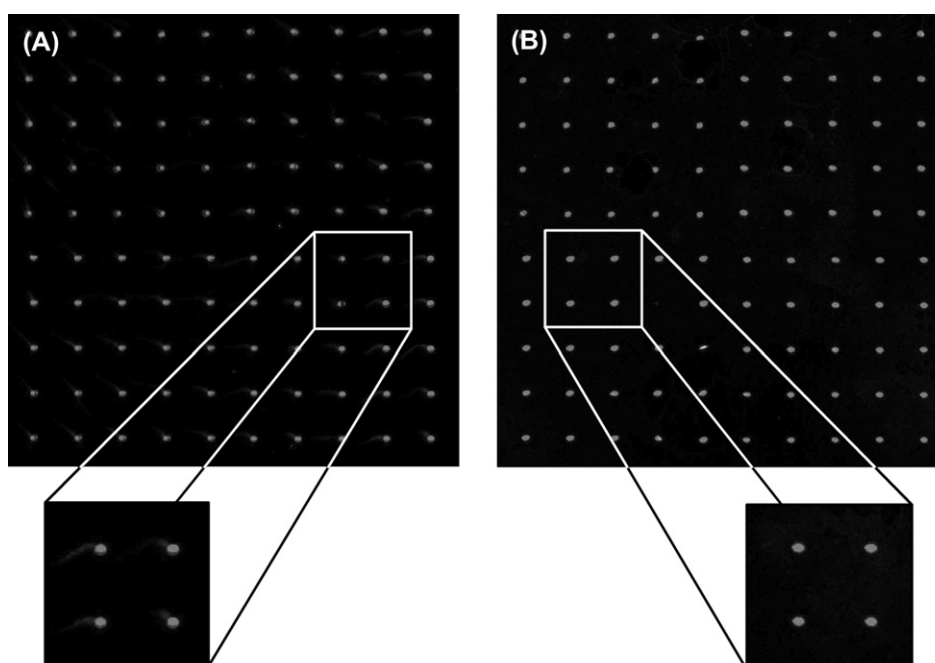


Fig. 9. Fluorescence microscopy image for (A) PolyIEMB-S-1% and (B) CO50-S-1%.

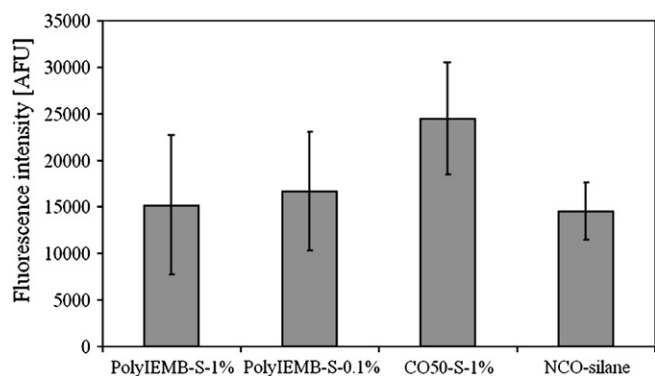


Fig. 10. Hybridization fluorescence intensity of PolyIEMB-S-1%, PolyIEMB-S-0.1%, CO50-S-1% and NCO-silane.

very similar (see Fig. 10). The background intensities for all the considered systems are quite low (mean \pm SD = 154 ± 10 AFU for PolyIEMB-S-1%, 326 ± 75 AFU for CO50-S-1%, and 144 ± 5 AFU for PolyIEMB-S-0.1%), and this allows obtaining a very good optical contrast of the deposition zone even for low fluorescence intensity.

Finally Fig. 9 gives also information about the shape of the spots, which is a valuable parameter of a high quality microarray. In particular CO50-S-1% coating shows well defined and circular spots: it allows a more accurate and quantitative evaluation of the fluorescence intensity through the scanner software, which approximates the spot to a dot. On the other hand, the PolyIEMB-S-1% system shows less regular spots with the presence of fluorescent tails that worsen the spot quality.

4. Conclusions

In this work a ketoxime blocked isocyanate methacrylic monomer (IEMB) was synthesized and copolymerized with *N,N*-dimethylacrylamide (DMA) in various compositive ratios. Some copolymers were dip-coated onto microscope glass slides obtaining highly functionalized and stable surfaces which are promising candidates for the fabrication of high quality microarrays.

The advantage of this approach is the prolonged shelf life of the device, and at the same time the NCO functionality can be restored by simply heating the glass slide just before use.

Preliminary tests were carried out in order to assess the binding and hybridization behavior of the new coatings during standard oligonucleotide's immobilization and recognition practices. Binding test results showed a good overall performance of the model devices prepared with an efficiency higher than those of silanized supports based on the same immobilization chemistry. The polymeric coatings permit to reach binding efficiency near to 100% for oligonucleotide concentration higher than 2.5 mM, while in the case of silanized surface the efficiency never reaches 70%. A substantial improvement in hybridization performances of the copolymer systems with respect to homopolymers and silanized surfaces was also observed, which could be related to an optimized balance among substrate adhesion, high degrees of freedom and functional group accessibility typical of macromolecular coatings.

Further points to be clarified are the apparent lack of adhesion of some coatings during the biotechnological processing of the microarray, and the need to optimize both molecular weight and composition of the copolymers for a complete compatibility of the new coatings with the microarray technology.

References

- [1] Schena M, Shalon D, Davis RW, Brown PO. *Science* 1995;270(20):467–70.
- [2] DeRisi JL, Iyer VR, Brown PO. *Science* 1997;278(24):680–6.
- [3] Van Hal NL, Vorst O, van Houwelingen AM, Kok EJ, Peijnenburg A, Aharoni A, et al. *J Biotechnol* 2000;78(3):271–80.
- [4] DeRisi J, Penland L, Brown PO, Bittner ML, Meltzer PS, Ray M, et al. *Nat Genet* 1996;14(4):457–60.
- [5] Heller RA, Schena M, Chai A, Shalon D, Bedilion T, Gilmore J, et al. *Proc Natl Acad Sci USA* 1997;94(6):2150–5.
- [6] Dufva M. *Biomol Eng* 2005;22(5–6):173–84.
- [7] Pirrung MC. *Angew Chem Int Ed* 2002;41(8):1276–89.
- [8] Pirrung MC. *Chem Rev* 1997;97:473–88.
- [9] Fodor SP, Read JL, Pirrung MC, Stryer L, Lu AT, Solas D. *Science* 1991;251:767–73.
- [10] Pease AC, Solas D, Sullivan EJ, Cronin MT, Holmes CP, Fodor SPA. *Proc Natl Acad Sci USA* 1994;91:5022–6.
- [11] McGall G, Fidanza JA. *Methods in molecular biology*. Totowa, NJ: Humana Press; 2001. p. 71–102.
- [12] Rose D. In: Schena M, editor. *Microarray biochip technology*. Natick: Eaton; 2000. p. 19–38.
- [13] Martinsky T, Haje P. In: Schena M, editor. *Microarray biochip technology*. Natick: Eaton; 2000. p. 201–20.
- [14] Mace Jr ML, Montagu J, Rose SD, McGuinness G. In: Schena M, editor. *Microarray biochip technology*. Natick: Eaton; 2000. p. 39–64.
- [15] Okamoto T, Suzuki T, Yamamoto N. *Nat Biotechnol* 2000;18:438–41.
- [16] Cooley P, Hinson D, Trost HJ, Antohe B, Wallace D. *Methods in molecular biology*. Totowa, NJ: Humana Press; 2001. p. 117.
- [17] Gong P, Grainger DW. *Surf Sci* 2004;570:67–77.
- [18] Benters R, Niemeyer CM, Drutschmann D, Blohm D, Wohlr D. *Nucleic Acids Res* 2002;30:e10.
- [19] Joos B, Kuster H, Cone R. *Anal Biochem* 1997;24:96–101.
- [20] Oh SJ, Cho SJ, Kim CO, Park JW. *Langmuir* 2002;18:1764–9.
- [21] Beier M, Hoheisel JD. *Nucleic Acids Res* 1999;27:1970–7.
- [22] Le Berre V, Trevisiol E, Dagkessamanskaia A, Sokol S, Caminade AM, Majoral JP, et al. *Nucleic Acids Res* 2003;31:e88.
- [23] Hong BJ, Oh SJ, Youn TO, Kwon SH, Park JW. *Langmuir* 2005;21:4257–61.
- [24] Wicks DA, Wicks Jr ZW. *Prog Org Coat* 1999;36:148–72.
- [25] Wicks DA, Wicks Jr ZW. *Prog Org Coat* 2001;43:131–40.
- [26] Wicks DA, Wicks Jr ZW. *Prog Org Coat* 2001;41:1–83.
- [27] Viganò M, Suriano R, Levi M, Turri S, Damin F, Chiari M. *Surf Sci* 2007;601:1365–70.
- [28] Sompuram SR, Vani K, Wei L, Ramanathan H, Olken S, Bogen SA. *Anal Biochem* 2004;326:55–68.
- [29] Fox TG. *Bull Am Phys Soc* 1956;1:123.
- [30] Couchman PR, Karasz FE. *Macromolecules* 1978;11:117.
- [31] Wicks Jr ZW, Jones FN, Pappas SP. *Organic coatings, science and technology*. 2nd ed. NY: Wiley; 1999.
- [32] Pierce PE, Schoff CK. *Coating film defects*. Blue Bell, PA: Federation of Societies for Coating Technology; 1988.
- [33] Wilson SK. *Surf Coat Int* 1997;80:162.
- [34] Cohu O, Magnin A. *Prog Org Coat* 1996;28:89–96.
- [35] Ngo AP, Cheever GD, Ottavini RA, Malinsky T. *J Coat Technol* 1993;65:29.
- [36] Barbier V, Viovy JL. *Curr Opin Biotechnol* 2003;14:51–7.
- [37] Schena M. *Microarray analysis*. Hoboken, New Jersey: Wiley; 2003.